

CR1g mediates early Kupffer cell responses to adenovirus

Jeannie Q. He,* Kenneth J. Katschke Jr.,* Peter Gribbling,* Eric Suto,* Wyne P. Lee,*
Lauri Diehl,[†] Jeffrey Eastham-Anderson,[†] Anusha Ponakala,* Laszlo Komuves,[†]
Jackson G. Egen,*^{1,2} and Menno van Lookeren Campagne*^{1,2}

Departments of *Immunology and [†]Pathology, Genentech, South San Francisco, California, USA

RECEIVED JUNE 28, 2012; REVISED OCTOBER 30, 2012; ACCEPTED NOVEMBER 14, 2012. DOI: 10.1189/jlb.0612311

ABSTRACT

Whereas adenoviral vectors are known to activate the complement cascade, leading to fixation of C3 proteins to the viral capsid, the consequences of this activation for viral clearance from the circulation are not known. Liver KCs, the macrophage population responsible for early uptake and elimination of many blood-borne pathogens, express CR1g, a complement receptor for C3 proteins. Here, we find that CR1g is important for the early elimination of C3-coated adenoviral vectors from the sinusoidal bloodstream by KCs. We further demonstrate that by acting as a critical receptor for adenovirus phagocytosis, CR1g plays an important role in regulating virus-induced KC death and depletion of these cells from the liver sinusoidal lumen. Our study thus identifies a critical pathway regulating KC function and survival in response to systemic viral infection. *J. Leukoc. Biol.* 93: 301–306; 2013.

Introduction

Hepatic KCs are the primary intravascular macrophage population in mammals and are responsible for clearance of many blood-borne pathogens from systemic circulation, including viruses. In the context of systemic adenoviral infections, KCs have been shown to play a critical role in uptake of adenovirus from the liver sinusoidal blood circulation and in shaping the initial antiviral innate immune response [1–3]. LSECs have also been implicated in viral uptake and in some instances, have been reported to be more important than KCs [4–6]. Indeed, receptors that have been implicated in adenovirus binding and uptake in the liver, such as scavenger receptors and FcRs, are expressed on KCs and LSECs [7].

Following phagocytosis of adenoviral particles, KCs undergo rapid cell death [3, 8]. This necrotic process is mediated by

adenovirus capsid protein VI, which is thought to directly disrupt cell membranes after being released during viral capsid disassembly [9]. As such, an adenovirus mutant strain *ts1*, whose capsid does not release the membrane lytic protein VI, enters normally into KCs but does not induce KC death [10]. Thus, loss of membrane integrity can be used as a sensitive readout of KC-adenovirus interactions and subsequent adenoviral uptake into intracellular compartments.

Adenoviral particles have been previously shown to induce complement activation through the alternative pathway [11]. This pathway leads to covalent attachment of C3 proteins (C3b and iC3b) to the adenoviral capsid, which could potentially serve as ligands for yet-to-be-defined receptors on macrophages [7, 12, 13]. However, the interplay between adenovirus and the complement system in vitro differs from that in vivo [14], and the specific molecular mechanisms underlying KC interactions with adenovirus particles in the blood have not been described in detail [3].

C3 proteins can mediate opsonization of pathogens and subsequent uptake by phagocytic cells through binding to one of two primary receptors—the integrin heterodimer CD11b/CD18 (complementary receptor 3, macrophage-1 antigen) or CR1g [15]. We have demonstrated previously that CR1g is expressed on KCs but not on splenic macrophages and plays a critical role in the host responses to systemic bacterial infections [16]. In this study, we investigate the role of CR1g in mediating early in vivo vascular responses to systemic adenoviral infection. We find that shortly following infection with a low dose of Ad5, circulating viral particles in the liver are captured and internalized by KCs into CR1g+ vesicles. With the use of intravital microscopy, we characterize the temporal and spatial dynamics of Ad5-induced loss of KC membrane integrity and demonstrate that CR1g, through interactions with C3 proteins, plays a critical role in regulating this early response to infection that culminates in KC death and loss from sinusoidal vessels. Thus, the presence of CR1g on KCs is required for rapid and efficient clearance of Ad5 from the circulation. However, CR1g-medi-

Abbreviations: Ad5=adenovirus serotype 5, C3=complement protein 3, CR1g=complement receptor Ig-superfamily, IHC=immunohistochemistry, KC=Kupffer cell, KO=knockout, LSEC=liver sinusoidal endothelial cell, Lys=lysozyme, mlgG1=mouse IgG1, PI= propidium iodide, qPCR=quantitative PCR

The online version of this paper, found at www.jleukbio.org, includes supplemental information.

1. Correspondence: Department of Immunology, Genentech, 1 DNA Way, South San Francisco, CA 94080, USA. E-mail: egen.jackson@gene.com or menno@gene.com
2. These authors contributed equally to this work.

ated viral uptake is also associated with a higher frequency of KC death, thereby rendering the host deficient in an important component of the innate immune response to systemic infection.

MATERIALS AND METHODS

Mice and antibodies

MHCII-GFP mice were described previously [17]. For LysM-GFP mice, animals expressing Cre recombinase under the LysM promoter [18] were crossed to the ACTB-Bgeo/GFP Cre reporter line [19]. C3 KO mice and CRIG KO mice were generated as described [16, 20]. All animals were held under sterile, pathogen-free conditions. Animal experiments were approved by the Institutional Animal Care and Use Committee of Genentech (South San Francisco, CA, USA). CRIG-blocking antibody 14G8 and -nonblocking antibody 25C5 were described previously [21].

Preparation of fluorescently labeled Ad5-lacZ and Ad5 infection

Ad5, a replication-incompetent human serotype 5, deleted for E1 and E3 expressing lacZ under the CMV promoter, were purchased from Vector Development Laboratory (Houston, TX, USA). To fluorescently label Ad5-lacZ, virus was mixed with Alexa Fluor (A) 647 dye (Invitrogen, Carlsbad, CA, USA) and 0.1 M sodium carbonate buffer for 30 min at room temperature, dialyzed, and stored in aliquots at -20°C . Titers were determined colorimetrically by infecting 293/E4 cells and staining with an anti-Ad5 polyclonal antibody (Access Biomedical, San Diego, CA, USA) and secondary goat anti-rabbit IgG conjugated with alkaline phosphatase. All viral infections were performed i.v. at a dose of 2.7×10^{10} pfu/kg, unless noted otherwise.

FACS analysis of KCs

WT and CRIG KO mice were i.v.-injected with Ad5-lacZ, and C3 WT or C3 KO mice were injected i.p. with 200 μg mIgG1 isotype control or CRIG-blocking antibody, 1 and 2 days before infection with Ad5-lacZ. At 18 h postinfection, livers were perfused with 4 ml HBSS/2 mM EDTA, followed by collagenase type IV treatment for 15 min. Nonparenchymal cells were isolated and stained with the LIVE/DEAD fixable dead cell stain kit (Invitrogen), F4/80-PE (eBioscience, San Diego, CA, USA), and anti-CRIG-A647 (clone 25C5) antibodies for flow cytometry analysis.

LDH measurements and quantifying Ad5 genomes

CRIG WT and KO mice were i.v.-injected with Ad5-lacZ, and 10, 30, and 60 min later, blood was harvested by cardiac puncture. Serum LDH was measured using the Liquid Lactate Dehydrogenase Reagent Set from Pointe Scientific (Canton, MI, USA). One international unit/liter is defined as the amount of enzyme that catalyzes the transformation of 1 μmol substrate/min. CRIG KO and WT mice were i.v.-injected with saline or Ad5-lacZ. Five minutes postinjection, mice were anesthetized with Nembutal. Blood was collected into EDTA-containing tubes, and livers were perfused with PBS and homogenized using a gentleMACS (Miltenyi Biotec, Germany). DNA was isolated using a DNeasy Blood & Tissue kit (Qiagen, Germantown, MD, USA), and viral genomes were quantified using Ad5-specific PCR primers as described [22] with normalization of viral genomes to GAPDH.

Intravital microscopy

Surgical preparation of the liver was performed as described [23]. Liver sinusoids were visualized by injecting Texas Red-conjugated BSA (Invitrogen) i.v., immediately prior to imaging. A tail vein catheter was used to administer virus or antibodies during imaging. Animals were imaged on a LSM 510 confocal imaging system (Carl Zeiss Microimaging, Thornwood, NY, USA) using visible laser excitation. Raw imaging data were processed with Imaris software (Bitplane, Switzerland) using Gaussian or edge-preserving filters.

For evaluating the effects of CRIG blockade on KC death, MHCII-GFP mice were injected i.p. with 200 μg mIgG1 control or CRIG-blocking antibody at 1 and 2 days before viral infection. Forty minutes after adenovirus infection, mice were administered PI, and images were captured from 10 randomly chosen regions of the liver. For evaluating the effects of Ad5 infection on KC membrane integrity, LysM-GFP mice were administered PI, followed by saline or Ad5 at the indicated time-points. Quantification of KC volume and the number of PI+ nuclei were performed using the Spots and Surfaces functions of Imaris (Bitplane), respectively.

IHC and confocal microscopy

For visualization of viral uptake by KCs, MHCII-GFP mice were infected with A647-labeled Ad5. Five minutes later, animals were sacrificed, and livers were fixed in paraformaldehyde, dehydrated in 30% sucrose, and embedded in OCT freezing media (Sakura Finetek, Torrance, CA, USA). Nuclei were labeled with Hoechst 33342 (Invitrogen). Images were captured using a Leica SPE confocal microscope (Leica Microsystems, Germany). Image-based quantification of Ad5-A647, which was associated with GFP+ KCs or with the surrounding GFP tissue, was performed by intensity thresholding of GFP and A647 fluorescence. Identical thresholds were applied to all images. A647+ pixels falling inside or outside of KC borders were calculated and expressed as a volume/imaging field. For examining bead uptake by KCs, animals were administered 2×10^8 1 μm diameter red fluorescent sulfate microspheres (Invitrogen) i.v., 40 min after Ad5 infection. Ten minutes after bead injection, livers were harvested, sectioned, and imaged as above. KCs and beads were quantified from four images/mouse and three mice/group. KCs were manually counted, and beads were quantified using the Spots function of Imaris software (Bitplane). For studies addressing colocalization of CRIG and Ad5, A647-labeled Ad5, followed 10 min later by A488-labeled anti-CRIG nonblocking antibodies, was injected i.v. into WT mice. Five minutes after antibody injection, livers were processed and imaged as described above. The number of A647-labeled Ad5 particles colocalized with CRIG+ vesicles versus adenovirus particles not colocalized with CRIG+ vesicles was counted manually in Z-stacks of confocal images obtained from five randomly selected KCs/animal ($n=3$). The average number of viral particles/KC was 11. For examining distribution of KCs in the livers of MHCII-GFP mice, livers were processed, stained with an A647-labeled anti-F4/80 antibody (eBioscience), and imaged as described above. For quantification of KC number using IHC, WT mice were i.v.-injected with various doses of Ad5-LacZ and injected i.p. with 200 μg mIgG1 control or CRIG-blocking antibody on the day before and the day of viral infection. At 18 h postinfection, livers were harvested, fixed in 10% formalin, and sectioned. KCs were stained with antibodies to F4/80 (Serotec, Raleigh, NC, USA) and visualized with DAB chromogen (Vector Labs, Burlingame, CA, USA). KCs were counted by applying standard morphological filters.

Statistics

Statistics were performed using GraphPad Prism 5 software (La Jolla, CA, USA). All *P* values were calculated using the two-tailed, unpaired *t*-tests, assuming unequal variance. *P* values ≤ 0.05 were considered significant.

RESULTS AND DISCUSSION

CRIG mediates clearance of viral particles from the circulation

Whereas KCs have long been considered the major cell responsible for rapid clearance of adenoviral particles from the bloodstream, a recent study has positioned LSECs as an important scavenger of adenovirus in the liver [4]. To determine the primary cell type in the liver responsible for adenoviral uptake in our system, we examined the localization of Ad5 particles shortly after infection. KCs were visualized in the sinusoidal lumen using mice in which the endogenous MHC class II pro-

tein was replaced with a fluorescently tagged version (MHCII-GFP) [17]. The relatively static GFP-expressing cells within the liver sinusoids of these animals have previously been shown to be composed of KCs [23]. MHCII-GFP animals were infected i.v. with A647-labeled Ad5 particles, and 5 min later, livers were perfused to remove any free virus within the circulation prior to fixation. Visualization of virus and KCs by confocal microscopy revealed that the majority of virus was internalized by KCs (Fig. 1A and B and Supplemental Video 1).

Whereas previous studies have shown that complement C3 enhances Ad5 uptake by KCs in the liver [13], it is not known which receptor mediates this process and to what extent complement C3 opsonization is important for Ad5 clearance. As CR1g is a complement C3b receptor with expression on all KCs in the liver, but absent on splenic MOMA- and F4/80-positive macrophages and alveolar macrophages [16], we hypothesized that CR1g may act as a KC receptor responsible for binding and internalization of C3-coated adenovirus particles in the blood. We infected CR1g WT and KO mice with Ad5 and examined the relative numbers of viral genomes in the blood by qPCR. Elimination of virus from blood was reduced in the absence of CR1g (Fig. 1C), indicating that CR1g acts as a clearance receptor for Ad5 particles in the circulation.

To determine whether Ad5 was associated with CR1g-positive vesicles upon phagocytosis by KCs [16, 21], mice were inoculated with A647-labeled Ad5 particles and subsequently administered A488-labeled nonblocking CR1g antibody i.v. to label recycling endosomes in KCs [16]. Fifteen minutes following infection, $47 \pm 12\%$ (mean \pm SD) of Ad5 particles colocalized with CR1g-positive endosomes in KCs (Fig. 1D, arrows). Particles that did not colocalize with CR1g may have escaped the endosome and entered the cytoplasm of the KC (Fig. 1D, arrowheads) [9]. Consistent with our earlier findings, only rarely were hepatocytes and LSECs infected (Supplemental Fig. 1A, arrowhead). These data suggest that CR1g mediates uptake of adenovirus particles by KCs, thus supporting efficient viral clearance from the circulation.

Early KC responses following adenovirus infection

KC phagocytosis of adenoviral particles has previously been shown to induce functional impairment of KCs and ultimately, cell death [3, 8, 9]. Surprisingly, continuous intravital imaging of liver sinusoidal beds in MHCII-GFP mice (Supplemental Fig. 1B) for up to 4 h following infection did not reveal any large-scale alterations in KC morphology or behavior (Supplemental Fig. 1C and Supplemental Video 2). However, 40 min following Ad5 infection, KCs showed a significant reduction in their ability to phagocytose i.v.-administered fluorescent beads (Fig. 2A and B), suggesting functional impairment.

Given that the MHCII-GFP mice express membrane-associated GFP, we reasoned that potential changes in membrane integrity as a result of Ad5 infection might not be apparent based on GFP fluorescence. Thus, we next examined KC responses to Ad5 infection using mice with cytoplasmic GFP expressed under the control of the LysM promoter (LysM-GFP) [18, 19]. These experiments revealed a synchronized loss of GFP from KCs, starting ~10 min after Ad5 infection (Fig. 2C and D and Supplemental Video 3). This loss of cytoplasmic

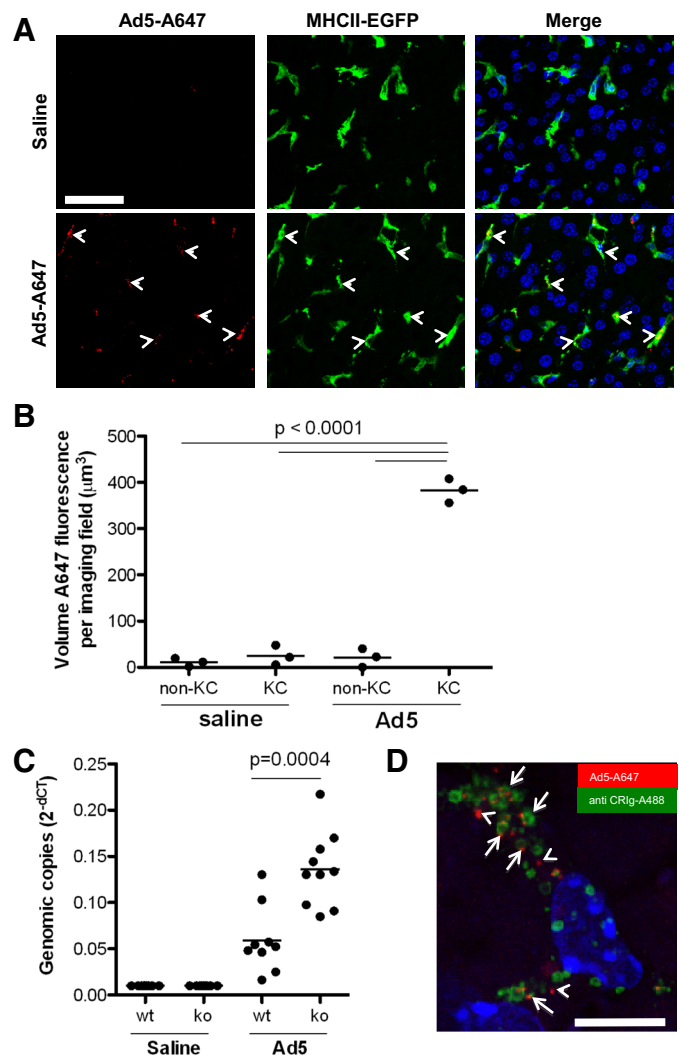


Figure 1. KCs and CR1g are involved in clearance of adenovirus from the circulation. (A) Representative confocal images of liver sections from the MHCII-GFP mice, 5 min postinfection with A647-labeled Ad5. Arrowheads indicate examples of Ad5 internalized by KCs. (B) Quantification of Ad5 uptake into KC and non-KC compartments of the liver. The volume of A647 fluorescence associated with GFP+ KCs or the surrounding tissue was quantified from images derived from three animals. A647 volume in saline-treated animals represents background fluorescence, which did not vary between compartments. (C) WT and CR1g KO mice were injected i.v. with saline or Ad5. Five minutes later, blood was collected, and relative genomic copies of Ad5 were determined by qPCR [expressed as $2^{-\Delta\text{cycle threshold (dCT)}}$]. (D) A647-labeled Ad5 was i.v.-injected into mice, followed 10 min later by injection of an A488-labeled nonblocking CR1g antibody to label recycling endosomes in vivo. Mice were taken down 5 min later, and liver was prepared for confocal analysis. Ad5 particles were associated with CR1g+ vesicles (arrows) but also appeared independent of CR1g+ organelles (arrowheads). A low-power magnification of this image is shown in Supplemental Fig. 1A. Original scale bars: (A) 40 μm ; (D) 10 μm .

GFP was paralleled by an increase in nuclear staining by PI, a cell-impermeant and nucleophilic dye that had been delivered i.v. prior to infection. Consistent with our results using the MHCII-GFP mice, despite losing membrane integrity following

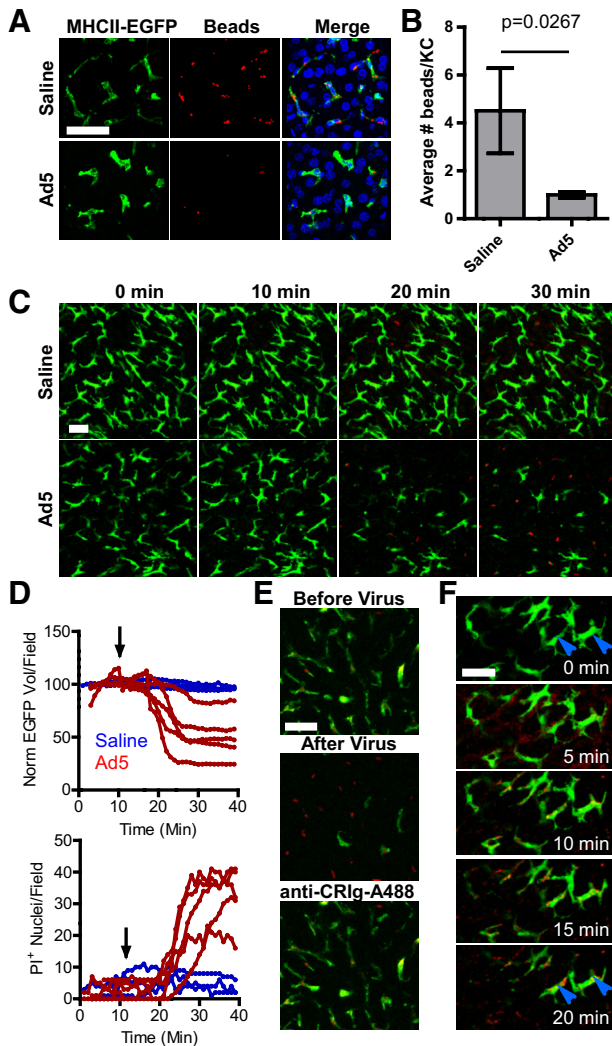


Figure 2. Early KC responses following adenovirus infection. (A) Representative images of liver sections from saline or Ad5-infected mice that were subsequently treated with fluorescent beads to evaluate KC phagocytosis capacity. (B) Quantification of beads and KC number from saline or Ad5-treated animals. Graph represents the average number of beads per KC \pm SD from three mice/group. Data are representative of two similar experiments. (C) Representative image series from LysM-GFP mice (green) that were injected with PI (red). Saline or Ad5 was administered 10 min after the start of imaging. Data are representative of four similar experiments. (D) Quantification of GFP loss and PI uptake in KCs following treatment with saline or Ad5 (arrows). The upper graph represents the change in GFP+ KC volume over time, normalized to the GFP+ cell volume over the first 10 min of imaging, and the lower graph represents the number of PI+ nuclei/imaging field over time. Each line on the graph represents an individual animal. (E) Representative image series from LysM-GFP mice (green) that were injected with PI (red) and subsequently infected with Ad5. Thirtyfive min later, after virus-induced KC death, animals were injected with A488-conjugated nonblocking CRlg antibody (green). (F) Representative image series from LysM-GFP mice (green) that were infected with A647-labeled Ad5 (red), 5 min after the start of imaging. Note that GFP is not lost in all KCs, despite uptake of virus (arrowheads). Experiments in D–F were repeated twice with similar results. (A, C, E, and F) Original scale bars: 40 μ m.

infection, KCs remained physically intact, as demonstrated by the ability of KCs that had lost cytoplasmic GFP expression to be labeled with an i.v.-injected, fluorescently tagged CRlg antibody (Fig. 2E and Supplemental Video 4). Of note, the failure of some KCs to lose membrane integrity following infection was not solely driven by exposure of the cells to virus, as throughout the liver, we observed KCs that had clearly ingested Ad5 but remained viable (Fig. 2F and Supplemental Video 5), potentially reflecting heterogeneity in the response of KCs to infection [24]. Hence, a rapid and synchronized loss

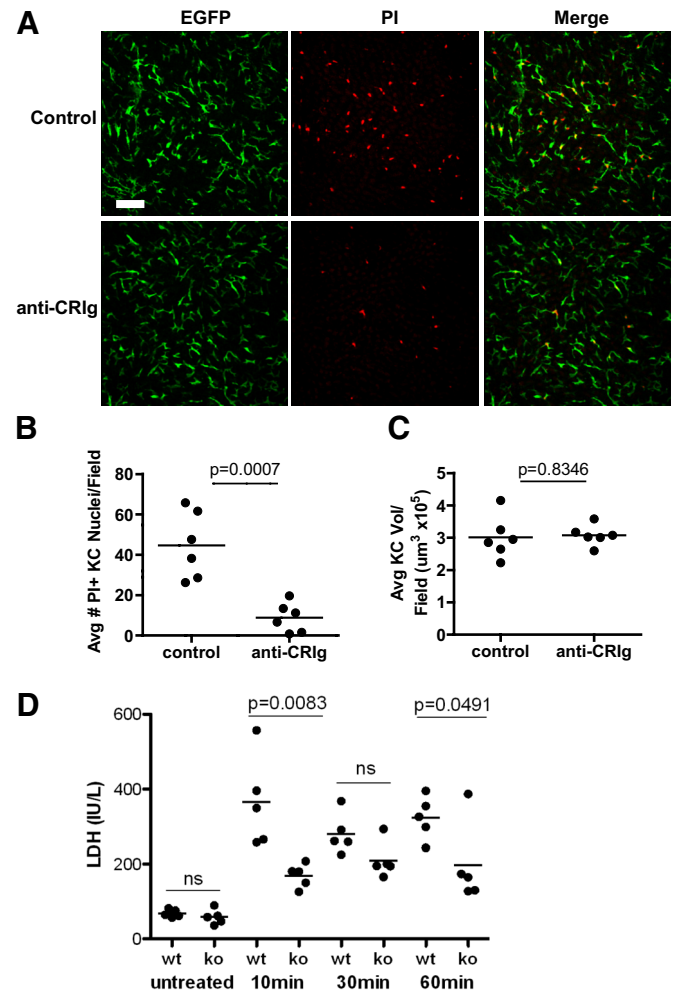


Figure 3. CRlg-mediated viral uptake by KCs induces rapid loss of KC viability. (A) Representative images from MHCII-GFP mice that had been pretreated with control or CRlg-blocking antibodies, injected with PI, and then infected with Ad5. Forty minutes after infection, images of the liver were captured by intravital microscopy. Original scale bar: 80 μ m. (B and C) The number of PI-positive KCs is reduced in MHCII-GFP mice treated with CRlg-blocking antibodies. Graphs represent the average number of PI+ cells/field (B) and the average KC volume/field (C). Each data point represents an individual mouse and was generated by averaging values from at least five randomly selected images of the liver/mouse. Data were compiled from three separate experiments. (D) Ablation of CRlg reduces the release of LDH into the serum following Ad5 infection. Experiments were repeated twice with similar results.

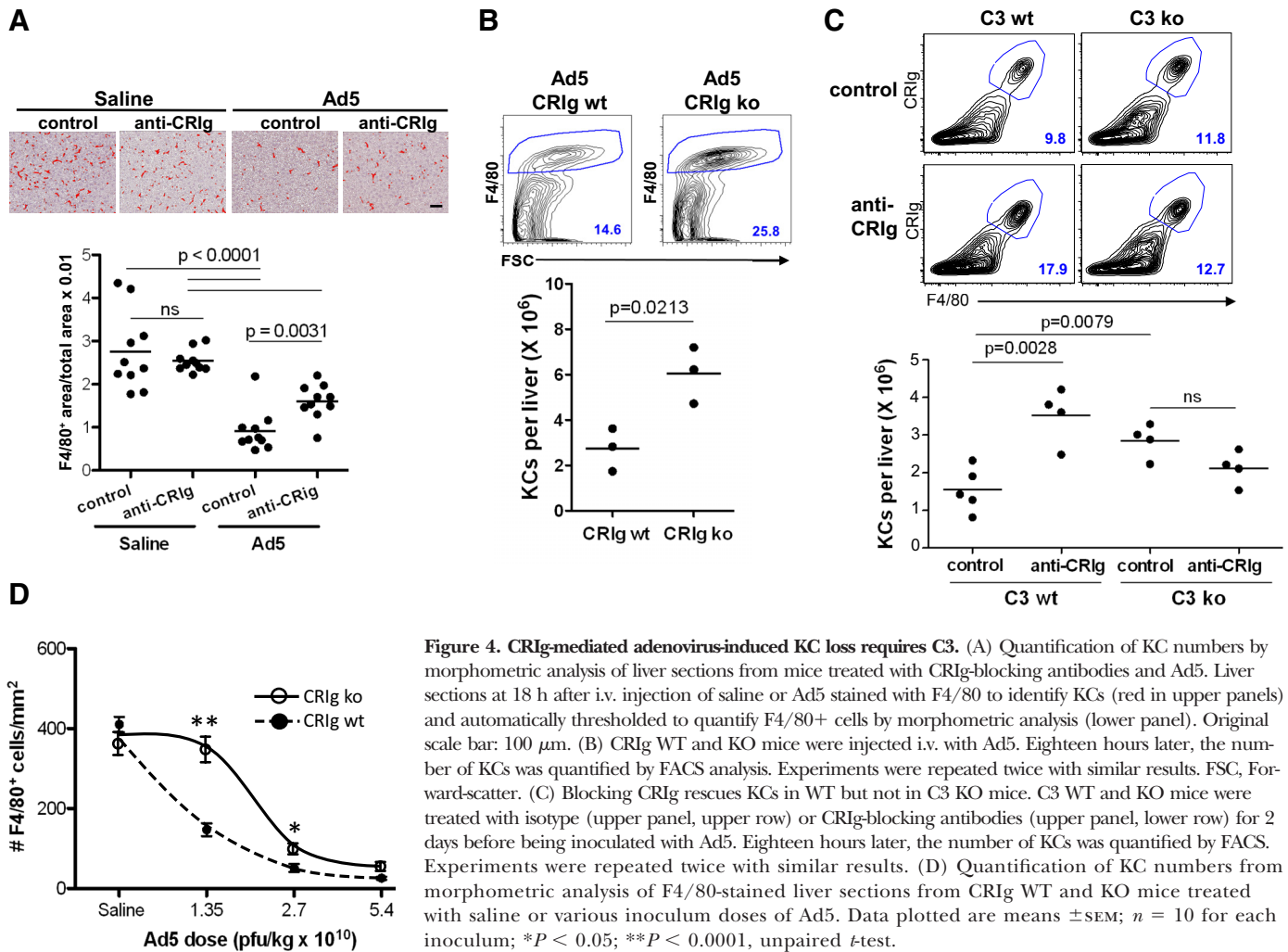


Figure 4. CRIg-mediated adenovirus-induced KC loss requires C3. (A) Quantification of KC numbers by morphometric analysis of liver sections from mice treated with CRIg-blocking antibodies and Ad5. Liver sections at 18 h after i.v. injection of saline or Ad5 stained with F4/80 to identify KCs (red in upper panels) and automatically thresholded to quantify F4/80+ cells by morphometric analysis (lower panel). Original scale bar: 100 μ m. (B) CRIg WT and KO mice were injected i.v. with Ad5. Eighteen hours later, the number of KCs was quantified by FACS analysis. Experiments were repeated twice with similar results. FSC, Forward-scatter. (C) Blocking CRIg rescues KCs in WT but not in C3 KO mice. C3 WT and KO mice were treated with isotype (upper panel, upper row) or CRIg-blocking antibodies (upper panel, lower row) for 2 days before being inoculated with Ad5. Eighteen hours later, the number of KCs was quantified by FACS. Experiments were repeated twice with similar results. (D) Quantification of KC numbers from morphometric analysis of F4/80-stained liver sections from CRIg WT and KO mice treated with saline or various inoculum doses of Ad5. Data plotted are means \pm SEM; $n = 10$ for each inoculum; * $P < 0.05$; ** $P < 0.0001$, unpaired t -test.

in KC viability and function dominates the early responses to systemic Ad5 infection.

CRIg-mediated adenoviral uptake induces rapid loss of KC viability

Given the rapid kinetics of KC death induced by Ad5 infection and the role of CRIg in mediating early clearance of blood-borne virus, we next examined the consequences of loss of CRIg function on KC-virus interactions. MHCII-GFP mice were treated with CRIg-blocking antibodies or control antibodies [21] prior to Ad5 inoculation, and intravascular PI was used to evaluate membrane permeability. Following systemic injection with Ad5, mice treated with CRIg-blocking antibodies showed a reduction in the number of PI-positive KCs compared with mice treated with control antibodies (Fig. 3A and B). Consistent with our earlier observations, the total number of KCs present within the liver sinusoids did not change following infection over these time periods (Fig. 3C). In line with these observations, genetic ablation of CRIg reduced Ad5-induced release of the cytoplasmic enzyme LDH into the circulation early after infection (Fig. 3D). These data indicate that CRIg is important for adenovirus recognition and phagocytosis by KCs, resulting in rapid KC death.

CRIg mediates C3-dependent KC loss from the liver sinusoids following adenovirus infection

To examine the consequences of CRIg-mediated Ad5 uptake and KC death at later time-points, we examined the frequency of KCs in the liver of mice 18 h after infection. As shown in Fig. 4A, Ad5 induced death of ~60% of KCs. Blocking CRIg resulted in sparing of ~45% of the KCs after infection, indicating that the remaining 55% of KC loss is not accounted for by CRIg but other KC-expressed receptors. Flow cytometry to quantify KC numbers in dissociated liver tissues confirmed that CRIg deficiency resulted in significant sparing of KCs in mice infected with Ad5 (Fig. 4B). Whereas lack of CRIg function affected Ad5-induced KC death, it did not result in greater infection of the liver, as Ad5-derived β -galactosidase expression in hepatocytes or liver extracts was similar between CRIg WT and KO animals (Supplemental Fig. 2A and B). These data suggest that additional mechanisms aside from CRIg-mediated adenovirus clearance or adenovirus-induced KC death are responsible for regulating the extent of hepatocyte infection.

We next examined whether CRIg-dependent interactions with Ad5 particles were mediated through opsonized C3b or iC3b by treating C3 WT and KO mice with CRIg-blocking or control anti-

bodies and measuring KC loss. In the absence of CRiG-blocking antibodies, C3 KO mice had significantly greater numbers of KCs compared with C3 WT mice following Ad5 infection ($P < 0.01$), demonstrating the importance of this pathway in adenovirus recognition by KCs and protection from KC death. Importantly, whereas CRiG blockade significantly prevented Ad5-induced KC loss in C3-sufficient mice ($P < 0.005$), it did not further rescue KCs in C3-deficient mice (Fig. 4C). These data suggest that CRiG and C3 are required for the efficient binding and endocytosis of adenovirus that ultimately leads to depletion of KCs from the liver sinusoidal lumen.

The experiments described in this study used a relatively low dose of virus (2.7×10^{10} pfu/kg) to examine CRiG-mediated adenovirus recognition by KCs. To determine whether CRiG's role in adenovirus uptake was influenced by viral dose, CRiG WT and KO mice were infected with multiple doses of Ad5, and KCs in the liver were quantified 18 h postinfection using morphometry. We observed that KCs were protected from death in CRiG KO mice at lower doses of virus but that this protection was lost as viral load increased (Fig. 4D). Combined with our earlier studies demonstrating partial, but not complete, prevention of Ad5-induced KC death in anti-CRiG-treated mice, these data suggest that other receptors, aside from CRiG, are also involved in KC-mediated adenovirus binding and internalization dependent on the inoculated dose of adenovirus [7].

Taken together, our studies demonstrate that CRiG plays an important role in regulating the efficiency by which systemic adenoviral infections are cleared by liver KCs and suggest that CRiG may be a key receptor for recognition and internalization of any virus that activates the complement pathway. Moreover, in the context of viral vector-based gene therapy approaches, CRiG blockade could prevent loss of KCs following inoculation of a low dose of adenovirus, while maintaining appropriate, albeit slower, systemic clearance of virus through CRiG-independent phagocytic pathways [7, 25].

AUTHORSHIP

J.Q.H., M.v.L.C., and J.G.E. conceived of and designed the experiments. J.Q.H., K.J.K., P.G., E.S., W.P.L., A.P., and J.G.E. performed the experiments. J.Q.H., J.E.A., L.D., and L.K. analyzed the data. J.Q.H., M.v.L.C., and J.G.E. wrote the paper.

ACKNOWLEDGMENTS

We thank R. Weimer, J. Tsai, and E. Ladi for helpful discussions.

DISCLOSURES

All authors are employees of Genentech. The authors have no other conflicting interests.

REFERENCES

- Aleman, R., Suzuki, K., Curiel, D. T. (2000) Blood clearance rates of adenovirus type 5 in mice. *J. Gen. Virol.* **81**, 2605–2609.
- Lieber, A., He, C. Y., Meuse, L., Schowalter, D., Kirillova, I., Winther, B., Kay, M. A. (1997) The role of Kupffer cell activation and viral gene expression in early liver toxicity after infusion of recombinant adenovirus vectors. *J. Virol.* **71**, 8798–8807.

- Smith, J. S., Xu, Z., Byrnes, A. P. (2008) A quantitative assay for measuring clearance of adenovirus vectors by Kupffer cells. *J. Virol. Methods* **147**, 54–60.
- Ganesan, L. P., Mohanty, S., Kim, J., Clark, K. R., Robinson, J. M., Anderson, C. L. (2011) Rapid and efficient clearance of blood-borne virus by liver sinusoidal endothelium. *PLoS Pathog.* **7**, e1002281.
- Jacobs, F., Wisse, E., De Geest, B. (2010) The role of liver sinusoidal cells in hepatocyte-directed gene transfer. *Am. J. Pathol.* **176**, 14–21.
- Snoey, J., Mertens, G., Lievens, J., van Berkel, T., Collen, D., Biessen, E. A., De Geest, B. (2006) Lipid emulsions potentially increase transgene expression in hepatocytes after adenoviral transfer. *Mol. Ther.* **13**, 98–107.
- Xu, Z., Tian, J., Smith, J. S., Byrnes, A. P. (2008) Clearance of adenovirus by Kupffer cells is mediated by scavenger receptors, natural antibodies, and complement. *J. Virol.* **82**, 11705–11713.
- Manickan, E., Smith, J. S., Tian, J., Eggerman, T. L., Lozier, J. N., Muller, J., Byrnes, A. P. (2006) Rapid Kupffer cell death after intravenous injection of adenovirus vectors. *Mol. Ther.* **13**, 108–117.
- Wiethoff, C. M., Wodrich, H., Gerace, L., Nemerow, G. R. (2005) Adenovirus protein VI mediates membrane disruption following capsid disassembly. *J. Virol.* **79**, 1992–2000.
- Smith, J. S., Xu, Z., Tian, J., Stevenson, S. C., Byrnes, A. P. (2008) Interaction of systemically delivered adenovirus vectors with Kupffer cells in mouse liver. *Hum. Gene Ther.* **19**, 547–554.
- Jiang, H., Wang, Z., Serra, D., Frank, M. M., Amalfitano, A. (2004) Recombinant adenovirus vectors activate the alternative complement pathway, leading to the binding of human complement protein C3 independent of anti-ad antibodies. *Mol. Ther.* **10**, 1140–1142.
- Murue, D. A., Petrilli, V., Zaiss, A. K., White, L. R., Clark, S. A., Ross, P. J., Parks, R. J., Tschopp, J. (2008) The inflammasome recognizes cytosolic microbial and host DNA and triggers an innate immune response. *Nature* **452**, 103–107.
- Zinn, K. R., Szalai, A. J., Stargel, A., Krasnykh, V., Chaudhuri, T. R. (2004) Bioluminescence imaging reveals a significant role for complement in liver transduction following intravenous delivery of adenovirus. *Gene Ther.* **11**, 1482–1486.
- Tian, J., Xu, Z., Smith, J. S., Hoffherr, S. E., Barry, M. A., Byrnes, A. P. (2009) Adenovirus activates complement by distinctly different mechanisms in vitro and in vivo: indirect complement activation by virions in vivo. *J. Virol.* **83**, 5648–5658.
- He, J. Q., Wiesmann, C., van Lookeren Campagne, M. (2008) A role of macrophage complement receptor CRiG in immune clearance and inflammation. *Mol. Immunol.* **45**, 4041–4047.
- Helmy, K. Y., Katschke K. J., Jr., Gorgani, N. N., Kljavin, N. M., Elliott, J. M., Diehl, L., Scales, S. J., Ghilardi, N., van Lookeren Campagne, M. (2006) CRiG: a macrophage complement receptor required for phagocytosis of circulating pathogens. *Cell* **124**, 915–927.
- Boes, M., Cerny, J., Massol, R., Op den Brouw, M., Kirchhausen, T., Chen, J., Ploegh, H. L. (2002) T-cell engagement of dendritic cells rapidly rearranges MHC class II transport. *Nature* **418**, 983–988.
- Clausen, B. E., Burkhardt, C., Reith, W., Renkawitz, R., Forster, I. (1999) Conditional gene targeting in macrophages and granulocytes using LysMcre mice. *Transgenic Res.* **8**, 265–277.
- Novak, A., Guo, C., Yang, W., Nagy, A., Lobe, C. G. (2000) Z/EG, a double reporter mouse line that expresses enhanced green fluorescent protein upon Cre-mediated excision. *Genesis* **28**, 147–155.
- Circolo, A., Garnier, G., Fukuda, W., Wang, X., Hidvegi, T., Szalai, A. J., Briles, D. E., Volanakis, J. E., Wetsel, R. A., Colten, H. R. (1999) Genetic disruption of the murine complement C3 promoter region generates deficient mice with extrahepatic expression of C3 mRNA. *Immunopharmacology* **42**, 135–149.
- Gorgani, N. N., He, J. Q., Katschke, K. J., Jr., Helmy, K. Y., Xi, H., Steffek, M., Hass, P. E., van Lookeren Campagne, M. (2008) Complement receptor of the Ig superfamily enhances complement-mediated phagocytosis in a subpopulation of tissue resident macrophages. *J. Immunol.* **181**, 7902–7908.
- Garnett, C. T., Erdman, D., Xu, W., Gooding, L. R. (2002) Prevalence and quantitation of species C adenovirus DNA in human mucosal lymphocytes. *J. Virol.* **76**, 10608–10616.
- Egen, J. G., Rothfuchs, A. G., Feng, C. G., Winter, N., Sher, A., Germain, R. N. (2008) Macrophage and T cell dynamics during the development and disintegration of mycobacterial granulomas. *Immunity* **28**, 271–284.
- Klein, I., Cornejo, J. C., Polakos, N. K., John, B., Wuensch, S. A., Topham, D. J., Pierce, R. H., Crispe, I. N. (2007) Kupffer cell heterogeneity: functional properties of bone marrow derived and sessile hepatic macrophages. *Blood* **110**, 4077–4085.
- Di Paolo, N. C., van Rooijen, N., Shayakhmetov, D. M. (2009) Redundant and synergistic mechanisms control the sequestration of blood-borne adenovirus in the liver. *Mol. Ther.* **17**, 675–684.

KEY WORDS:

complement • phagocytosis • liver sinusoidal endothelial cell • Intravital microscopy • cell death • innate immunity • infection